

Title	Thermal Molecular Motion Can Amplify Intermolecular Magnetic Interactions
Author(s)	Uchida, Yoshiaki; Watanabe, Go; Akita, Takuya et al.
Citation	Journal of Physical Chemistry B. 2020, 124(28), p. 6175-6180
Version Type	AM
URL	https://hdl.handle.net/11094/91499
rights	This document is the Accepted Manuscript version of a Published Work that appeared in final form in The Journal of Physical Chemistry B, ©2020 American Chemical Society after peer review and technical editing by the publisher. To access the final edited and published work see https://doi.org/10.1021/acs.jpcc.0c05408 .
Note	

Osaka University Knowledge Archive : OUKA

<https://ir.library.osaka-u.ac.jp/>

Osaka University

Thermal Molecular Motion Can Amplify Intermolecular Magnetic Interactions

Yoshiaki Uchida, Go Watanabe, Takuya Akita, and Norikazu Nishiyama*

Graduate School of Engineering Science, Osaka University, Toyonaka, Osaka, JAPAN 560-8531

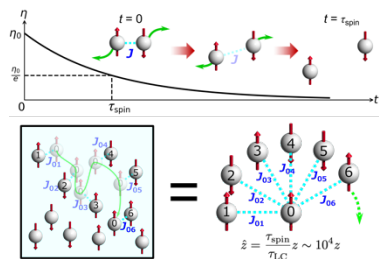
School of Science, Kitasato University, JAPAN 252-0329

Corresponding Author

* yuchida@cheng.es.osaka-u.ac.jp.

Abstract: Against a sensible expectation that molecular mobility in fluids generally disrupts magnetic orderings that depend on intermolecular interactions, some molecular compounds with isolated electrons, which are called radicals, exhibit the increase of magnetic susceptibility in melting. Here we first propose a simple model to explain the thermomagnetic anomaly unique to fluids; the effect of the magnetic interactions in each of the contacts could be accumulated on each of the molecular spins as if the molecular motion amplified the first coordination number of each molecule hundredfold. The huge coordination number theoretically guarantees the retention of memory of interactions at equilibrium; molecules might be able to conserve the memory of molecular conformations, configurations, electric charges, energies as well as magnetic memory with each other.

TOC GRAPHICS



KEYWORDS: Intermolecular interactions, Molecular motion, Liquid crystals, Mean field theory, Retention times.

1. Introduction

A fast-moving molecule in fluids randomly contacts with other molecules one after another as illustrated in Figure 1.¹ When the molecule can maintain the influence of the contacts, the influence could migrate among the molecules in non-equilibrium states; e.g., photon upconversion effectively occurs when a triplet excited state can migrate through the acceptors in a solution.² Under the right conditions, the migratable memory might be conserved even at equilibrium. As one of the conservable memories, spin polarization is able to transfer between molecules;³ meanwhile, molecular motions are also, paradoxically, expected to disrupt any magnetic orderings due to relaxation. Spin exchange interactions, spin-orbit coupling or electric conduction is generally essential to inhibit the disruption of magnetic ordering because magnetic-field-induced magnetic moment of an isolated electron spin rapidly relaxes. To conserve the magnetic moment in crystalline (Cr) phases at room temperature, spin exchange interactions in 1-D and in 2-D are not enough and impracticably strong spin exchange interactions in 3-D are necessary as illustrated in Figure 1(a)-(d). However, the interaction is extremely weak for

nitroxide radicals (NRs), and therefore, even their ferromagnetic Cr phases show the ferromagnetic transitions at extremely low temperature no more than 1.48 K.⁴ In contrast to the history of the molecular magnetism of all-organic crystals, non-conductive NRs have proven to show unique magnetic properties in their liquid crystalline (LC) and isotropic liquid phases; magnetic susceptibilities abruptly increase in melting. It is called positive magneto-LC effect.⁵ Given the fact that the magnetic moment of NRs can magnetically interact only with their adjacent molecules, the mechanism of the magnetic property unique to fluids has proven elusive.

At first, magneto-LC effects were reported to arise simply from inhomogeneous intermolecular magnetic interactions on the analogy of the magnetic ordering in spin glasses.⁶ Meanwhile, other experimental results indicate that molecular mobility is another origin of magneto-LC effects;⁷ it evokes the effects of the dynamics on the magneto-LC effects. We focused on the difference in magnetization behaviors between two categories of magnetic molecular LC materials: metallomesogens and LC organic radicals.⁸ The former does not show magneto-LC effects, whereas the latter does as mentioned above. First, spin-lattice relaxation time (T_1) of organic radicals ($10^{-7} \sim 10^{-5}$ s) is generally much longer than that of metal ions ($10^{-12} \sim 10^{-8}$ s);^{9, 10} retention time of the incremental magnetic field (η) induced by the spin-spin interaction between a certain pair of spins (τ_{spin}) illustrated in Figure 1(e) should be much longer for LC organic radicals than metallomesogens. Second, retention time of the spin-spin interaction should be the same as that of the intermolecular contact in the LC phase (τ_{LC}), which naturally depends on molecular diffusion. Therefore, the retention times of the spin-spin interaction of LC organic radicals are generally shorter than that of high-viscosity metallomesogens. Given the expectation that the number of the interactions during τ_{spin} should be larger in LC organic radicals than in metallomesogens; the magneto-LC effects originate from the conservation of the memory of the

spin-spin interactions between magnetic moments owing to the ceaseless molecular contacts as shown in Figure 1(f). Here, we propose a quantitative model incorporating the inhomogeneity of the magnetic interactions based on Thouless-Anderson-Palmer (TAP) approach,^{11, 12} which was proposed to solve Edwards-Anderson model for spin-glasses with inhomogeneous magnetic interactions,¹³ with careful consideration of characteristics of fluid phases and a spin localized in each molecule. And we discuss the validity of the new model by means of molecular dynamics (MD) simulation and density functional theory (DFT) calculations.

2. Methods

2.1. Molecular Dynamics Simulation

All-atom MD simulation was carried out using the MD program GROMACS 4.6.6. The partial atomic charges of the simulated LC molecule were determined by the restrained electrostatic potential (RESP)¹⁴ methodology at the UB3LYP/6-31G(d,p) level using the GAUSSIAN 09 package.¹⁵ In order to calculate the intra- and intermolecular interactions, generalized Amber force field¹⁶ parameters were used.

The initial structure of the MD simulation system was the cubic simulation box with the side of 8.0 nm containing 1024 molecules by replicating the small rectangular cell containing both enantiomers with random rotation. Based on the Cr structure obtained from the experiment for (2*S*,5*S*)-enantiomer,¹⁷ both (2*S*,5*S*)- and (2*R*,5*R*)-enantiomers were placed in the small rectangular unit cell as shown in Figure S1. The relaxation runs at 300 K for 10 ns and at 400 K for 30 ns were successively performed. During the relaxation runs, the Berendsen thermostat and barostat¹⁸ were used to keep the temperature and pressure of the system with relaxation times of 0.2 and 2.0 ps, respectively. After the relaxation runs, the equilibration run at 400K was done for 100 ns using Nosé-Hoover thermostat¹⁹ and Parrinello-Rahman barostat²⁰ with relaxation times of 1.0 and 5.0

ps, respectively. The time step was set to 2 fs since all bonds connected to hydrogen atoms were constrained with the LINCS algorithm.²¹ The smooth particle-mesh Ewald (PME) method was employed to treat the long-rang electrostatic interactions and the real space cutoff and the grid spacing are 1.4 and 0.30 nm, respectively.

A snapshot of MD simulation shown in Figure S2 shows that LC molecules tend to align along one direction after 100 ns of the equilibration run. For the quantitative analysis of the orientational order for LC molecules, we calculated the nematic order parameter. The nematic order parameter was estimated as the largest positive eigenvalue of the order parameter tensor \mathbf{P} , as expressed below:

$$P_{\alpha\beta} = \frac{1}{N} \sum_{i=1}^N \frac{1}{2} (3n_{i\alpha}n_{i\beta} - \delta_{\alpha\beta})$$

where N is the total number of LC molecules, subscripts α and β represent the coordinates x , y , and z . \mathbf{n}_i is the normalized vector of the i th molecular long axis defined as the vector connecting the two end carbon atoms in the rigid aromatic core part as shown in the inset of Figure S3. As shown in the time profile of the nematic order parameter for the system, the system reached equilibrium after 50 ns. The average order parameter during the last 20 ns was 0.71 ± 0.01 and indicates that the simulated system was in the nematic LC state. The mean square displacement (MSD) of the LC molecules was analyzed as shown in Figure S4. The self-diffusion coefficient calculated by using the Einstein relation was $2.02 \times 10^{-11} \text{ m}^2/\text{s}$ and the system has fluidity to the same extent as typical nematics.²² The radial distribution function (RDF) of the center of the mass of the LC molecules was also analyzed. The RDF, $g(r)$, is defined as

$$g(r) = \frac{1}{4\pi r^2 \Delta r} \frac{V}{N} \frac{1}{N} \sum_{i=1}^N \Delta N_i(r)$$

where V is the total volume of the system, N is the total number of the LC molecules, $\Delta N_i(r)$ is the number of the LC molecules in the shell at a distance r from the i th molecule, and Δr is the thickness of the shell. In Figure S5, $g(r)$ does not exhibit discrete sharp peaks and it is the characteristics of the typical fluids.

2.2. DFT Calculation for one of Snapshot Geometries of Molecular Dynamics Simulation

We extract molecular pairs that are effectively interacting with each other by choosing the pairs with which the distance between their centers of gravity is less than 1 nm. Actually, we select 1807 pairs of molecules. Single-point calculation of energies of singlet and triplet states, $E_{ij,\text{Singlet}}$ and $E_{ij,\text{Triplet}}$, was performed for all the 1807 pairs at the UB3LYP/6-31G(d,p) level using the GAUSSIAN 09 package.¹⁵ We define that J_{ij} is singlet-triplet gap in Joule, $E_{ij,\text{Singlet}}$ and $E_{ij,\text{Triplet}}$ are the energy in singlet and triplet states of the pair of molecules i and j , respectively.²³⁻²⁵

3. Results and Discussion

First, we derive the relation between magnetic susceptibility and magnetic interactions in fluid phases of molecules. All magnetic interactions involving the magneto-LC effects are described based on the interaction Hamiltonian of Edwards-Anderson model;

$$H = - \sum_{i,j} J_{ij} \mathbf{S}_i \mathbf{S}_j \quad (1)$$

where \mathbf{S}_i denotes the spin of molecule i interacting with molecule j with a random set of exchange couplings (J_{ij}). To introduce the inhomogeneity of the magnetic interactions in LC phases, we assume that each of the J_{ij} values is decided independently from a Gaussian probability density with mean zero, in which the mean field is not induced simply by the surrounding spins on average as the first-order term, and variance J^2/N in LC phases;

$$P(J_{ij}) \propto \exp\left(-\frac{NJ_{ij}^2}{2J^2}\right) \quad (2)$$

where N denotes the numbers of the molecules. According to the TAP approach, the non-zero variance (J^2/N) indicates that the incremental magnetization of the spins interacting with spin \mathbf{S}_i induced by spin \mathbf{S}_i recursively influences \mathbf{S}_i as the second-order term; the mean field was divided into two terms.

$$\mathbf{h}_i = \mathbf{h}_i^0 + \eta \mathbf{S}_i \quad (3)$$

where the first term, \mathbf{h}_i^0 , is the field that would be present in the absence of the spin \mathbf{S}_i (retaining the couplings J_{ij}), and the second term, $\eta \mathbf{S}_i$, is the recursive contribution of the spins interacting with \mathbf{S}_i , when \mathbf{S}_i is introduced. Note that the first-order term of $\eta(J_{ij})$ is canceled out because the average of J_{ij} is zero. Meanwhile, the second-order term $\eta(J_{ij}^2)$ in the three-dimensional vector spin model can be derived according to the approach with a hole that Palmer proposed.¹²

$$\eta = \frac{2}{3} \frac{1}{\Delta E} \sum_j J_{ij}^2 \quad (4)$$

When that external magnetic field, H_0 , is constant and enough larger than the mean field, ΔE can be approximated to be $g\mu_B H_0$, which is Zeeman energy. For spin glasses, in which coordination number is assumed to be N , the summation of J_{ij}^2 is J^2 . Meanwhile, for LC phases of NRs, the normal coordination number z is much smaller than N due to the bulkiness of the NRs as shown in Figure 1(a), and therefore, the summation of J_{ij}^2 is estimated to be zJ^2/N . Since J^2/N is the variance of J_{ij} and the J^2/N for the LC-NRs is expected to be much smaller than that for the ordinary spin glasses, this model is not likely to rationalize the magneto-LC effect in the higher temperature ranges. It suggests that just introducing the inhomogeneity is not enough to explain the magneto-LC effect. To also consider the effect of molecular mobility, we convert z into the

effective coordination number \hat{z} ; molecules exchange their interaction partners many times in τ_{spin} as if a molecule shared the spin polarization induced by the interactions with another molecule to other molecules before forgetting it as illustrated in Figure 1(f).

$$\sum_j J_{ij}^2 = \frac{\hat{z}}{N} J^2 \quad (5)$$

The strength and frequency of the molecular contact are $\exp(-t/\tau_{\text{spin}})$ and $1/\tau_{\text{LC}}$, respectively.

We can assume that \hat{z} depends on the above-mentioned two time periods: τ_{spin} and τ_{LC} .

$$\hat{z} = \int_0^\infty \frac{e^{-\frac{t}{\tau_{\text{spin}}}}}{\tau_{\text{LC}}} z dt = \frac{\tau_{\text{spin}}}{\tau_{\text{LC}}} z \quad (6)$$

The mean field for spin i described as eqs 3-6 leads to the following Curie-Weiss type equation with Weiss constant θ for the LC phases of NRs (θ_{LC}); we assume that this approximation should be plausible in such a high temperature region, in which LC phases of NRs are stable.⁵⁻⁷

Paramagnetic susceptibility in the LC phases (χ_{LC}) can be estimated using the obtained θ_{LC} .

$$\chi_{\text{LC}} = \frac{C}{T - \theta_{\text{LC}}} = \frac{C}{T - \frac{\hat{z}}{N} \frac{J^2}{6kg\mu_B H_0}} \quad (7)$$

where k is Boltzmann constant. If the Cr phase has no effective exchange interactions ($\theta_{\text{Cr}} = 0$) like typical LC-NRs, we can compare χ_{LC} with the susceptibility of the Cr phase, χ_{Cr} , at the melting point ($T \gg \theta_{\text{LC}}$).

$$\frac{\chi_{\text{LC}}}{\chi_{\text{Cr}}} = \frac{1}{1 - \frac{\hat{z}}{N} \frac{J^2}{6kg\mu_B H_0 T}} \simeq 1 + \frac{\hat{z}}{N} \frac{J^2}{6kg\mu_B H_0 T} \quad (8)$$

This equation is qualitatively consistent with reported H_0 -dependence of χ_{LC}/χ_{Cr} for LC-NRs; this ratio generally decreases as H_0 increases for positive magneto-LC effect.⁶ Numerical simulation of \hat{z} and J^2/N would enable us to quantitatively confirm the validity of this equation.

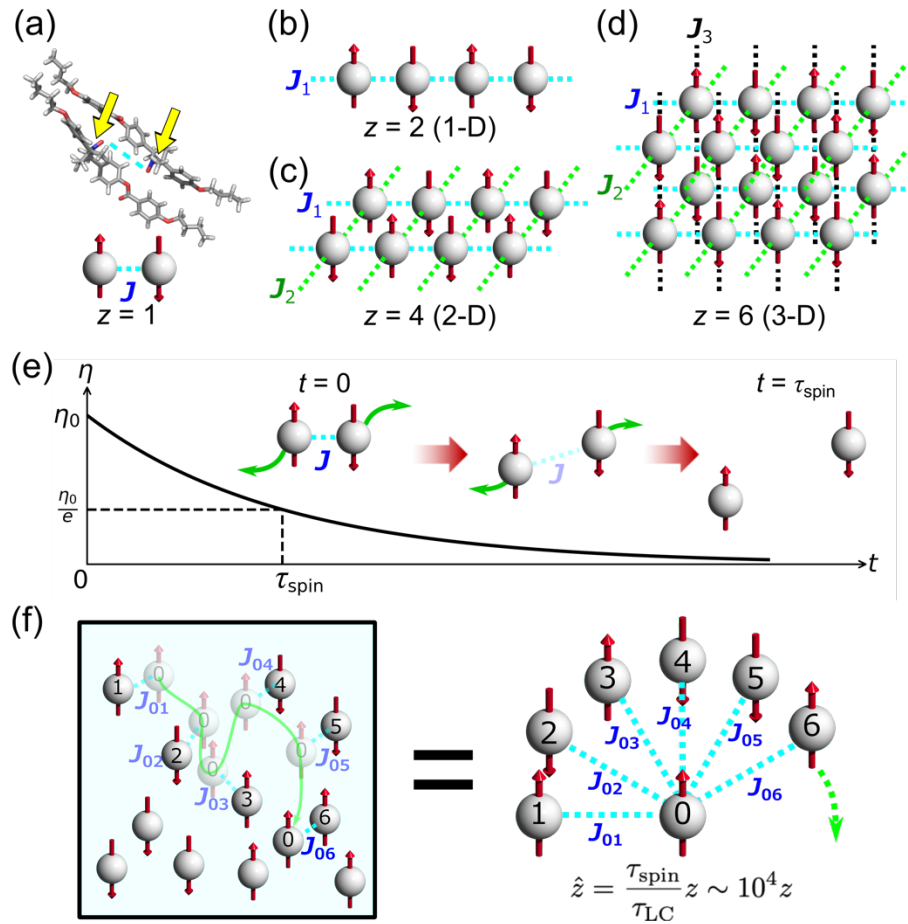


Figure 1. High-frequency exchange of interacting pairs detectable as increase of coordination number. (a) Molecules interact with each other in fluids. Because LC-NR molecules are bulky, each of them usually interacts with only one other molecule. In this case, the coordination number z is 1. (b)-(d) Generally speaking, z values for one, two and three-dimensionally interacting NR crystals are 2 (b), 4 (c) and 6 (d), respectively. (e) Schematic illustration of the

attenuation of η for a certain pair of molecules. The horizontal axis denotes the time elapsed since the interaction occurs. After a molecule interact with another molecule, it moves and the interaction disappears. The effect of the exchange magnetic field disappears after time constant τ_{spin} . (f) Each molecule changes the partner of the interaction many times before disappearance of the effect of the exchange magnetic field. Each molecule interacts with a lot of molecules as if coordination number substantially increased (\hat{z}).

Instead of X-ray crystallography for the analysis of the interacting manner of ordinary crystalline magnetic materials, we perform molecular dynamics (MD) simulation for 4NO4, which is the smallest one of the first generation chiral LC-NRs abbreviated to *mNO_n* as shown in Figure 2(a), to directly estimate τ_{LC} and the obtained configuration of the intermolecular interactions was used to estimate J^2/N . As is often the case with MD simulation of LC materials, the calculation started from random configuration of 1024 molecules of racemic 4NO4 prepared from real Cr structure of one of the enantiomers of 4NO4 (See Supporting Information); the magneto-LC effects have been well investigated for them.⁵⁻⁸ The density of the system is set to be 1 g cm^{-3} . We measured a period during the distance, d , between oxygen atoms of nitroxide moieties in adjacent molecules smaller than 1 nm, which is the limit of intermolecular distances between radical species with a localized spin to magnetically interact with each other,²⁶ to be 0.22 ns at 400 K as shown in Figure 2(b),(c). We assume the period is nearly equal to τ_{LC} ; it is consistent with generally estimated rotational and translational correlation times for LC phases $10^{-10} \sim 10^{-9} \text{ s}$.^{27, 28}

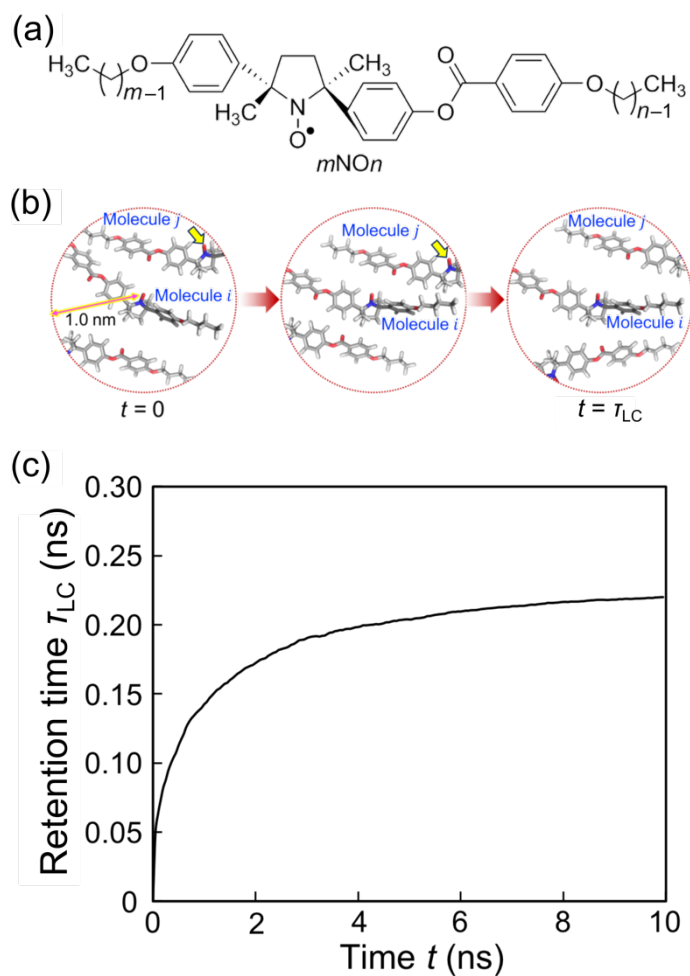


Figure 2. Molecular motion analysis for molecular configurations obtained from molecular dynamics simulation. (a) Molecular structures of *mNO_x*. (b) Schematic of the definition of the retention time τ_{LC} . Red circles denote 1 nm distant from molecule *i*. Time required from the entering of molecule *j* into the circle to the leaving of the same molecule from the circle is defined as τ_{LC} . (c) The time course of τ_{LC} . Although τ_{LC} is initially very low because all molecules initially exist inside the red circle shown in (b), it is likely to converge to 0.22 ns over time.

Next, we have performed DFT calculations for the configuration obtained from the above-mentioned MD simulation to estimate J^2/N . In a certain configuration, there are 1807 molecular pairs with the distance, d , less than 1 nm. We calculated J_{ij} as the difference between single point energies for singlet and triplet of each of the 1807 pairs (See Supporting Information),²⁶ and the histogram of J_{ij} shows that the number of the pairs around $J_{ij} = 0$ is quite large, indicating that most pairs do not interact with each other. When we assume that the dispersion obeys a Gaussian function, we can fit it with an equation with standard deviation $J = 1.1 \times 10^{-22}$ J. Note that the two points closest to $J_{ij} = 0$ were eliminated for the fitting because they involve some of the distant pairs without any interactions. The integration of the function indicate that the number of the interacting pairs is only 182 as shown in Figure 3(a), from which z can be estimated to be 0.355. As a lot of papers reported, we assumed that the spin-lattice relaxation time (T_1) of NRs is generally $10^{-7} \sim 10^{-6}$ s at such a high temperature. If τ_{spin} is comparable to T_1 , \hat{z} is estimated to be $1.6 \times 10^2 \sim 10^3$. If $g\mu_B H_0$ is 6.1×10^{-24} J in 3300 Oe that is the usual magnetic field for X-band electron paramagnetic resonance (EPR) spectroscopy and kT is 5.5×10^{-21} J at 400 K, we can estimate using eq 7 that the increase of the magnetic susceptibility in melting is 1.2% \sim 12%. In fact, X-band EPR spectroscopy with 3300 Oe around 400 K has recognized the magneto-LC effects up to a few tens % jump of magnetic susceptibility.^{5, 6} In addition, we estimated magnetization curves for $\tau_{\text{spin}} = 1.0, 0.5$ and $0.1 \mu\text{s}$ in the ranges of $H_0 < -1000$ Oe and $H_0 > 1000$ Oe because the approximation is valid for the high magnetic field as shown in Figure 3(b). This leads to the decrease of the ratio $\chi_{\text{LC}}/\chi_{\text{Cr}}$ with increasing H_0 , which is consistent with the experimental results for positive magneto-LC effect.⁶ These indicate that the model is valid for the magneto-LC effect of LC-NRs. Rapidly rotating or diffusing LC-NRs could show stronger magneto-LC effects.

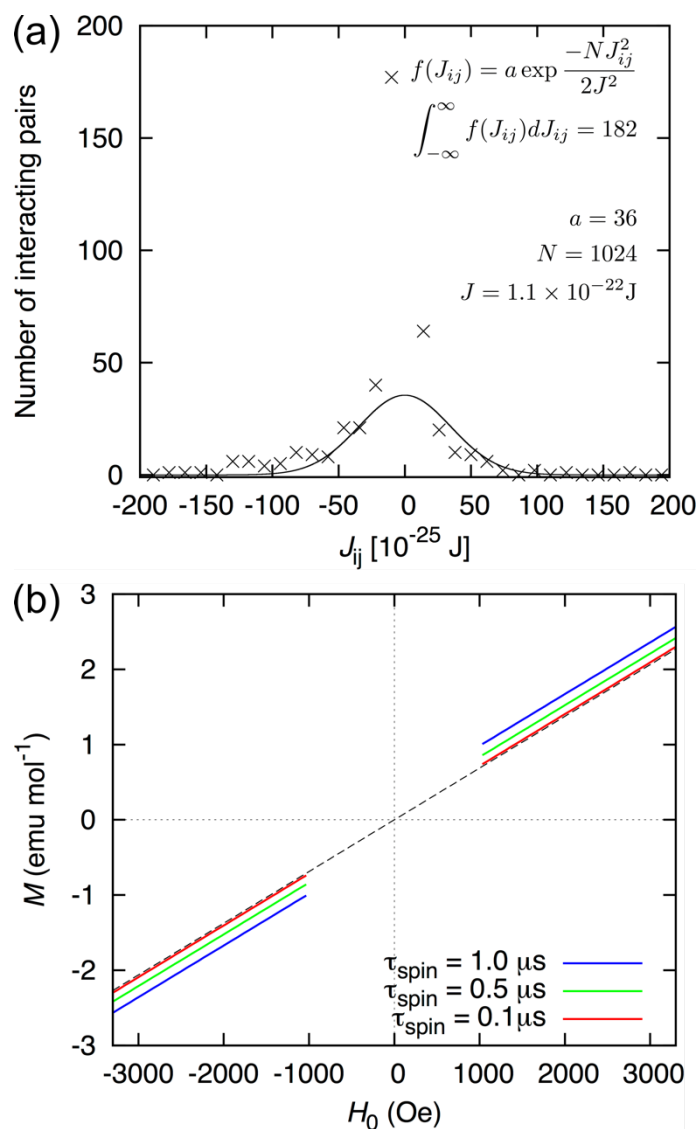


Figure 3. Simulated magnetic properties. (a) Distribution of J_{ij} obtained from DFT calculation results. The crosses denote the simulated values, and the solid line denotes the fitting line. (b) Magnetization curves depend on τ_{spin} . Dashed line denotes paramagnetic magnetization without any magnetic interactions. Red, green and blue curves denote magnetization curves with τ_{spin} of 0.1, 0.5 and 1.0 μs , respectively.

4. Conclusions

Our theory has successfully accounted for the positive magneto-LC effect in terms of the molecular mobility and inhomogeneity of intermolecular interactions; the estimated magnetic susceptibility is consistent with the previously reported experimental results. This is one of the scenarios to explain the emergence of the magneto-LC effects. Further examinations will tell how valid the theory is. In addition, a molecule with photoexcited triplet electrons might be able to further enhance the spin polarization of LC molecules owing to radical-triplet pair mechanism.²⁹ Our theory differs from mean field theories for magnetism with static interactions in the concept that molecular mobility can amplify the contact frequency; the theoretically estimated coordination number is $10^2 \sim 10^4$. Molecules might be able to conserve the memory of molecular conformations, configurations, electric charges, energies as well as magnetic memory with each other. As well as the theories for static interactions applied for any other sciences, our theory could be extended into systems with dynamic changes in the interactions between components; e.g., neurons, persons and economic players have such interactions with each other in a neuronal system, a community and a business world, respectively.³⁰

Supporting Information. The following files are available free of charge.

Detailed methods of Molecular Dynamics Simulation and Density Functional Theory Calculations (PDF)

Notes

The authors declare no competing financial interests.

ACKNOWLEDGMENT

We thank Prof. M. Negoro, Prof. Y. Kitagawa, Prof. T. Araki, Prof. T. Yokoyama, Prof. N. Nakano and Prof. R. Tamura for helpful advice. The computations were partly performed using Research Center for Computational Science, Okazaki, Japan. This work was supported by JSPS KAKENHI Grant Numbers JP17H04896, JP19H05718 and JP20H05161.

REFERENCES

- (1) Einstein, A. Über die von der molekularkinetischen Theorie der Wärme geforderte Bewegung von in ruhenden Flüssigkeiten suspendierten Teilchen. *Ann. Phys.* **1905**, 322, 549-560.
- (2) Parker, C. A.; Hatchard, C. G. Sensitised anti-stokes delayed fluorescence. *Proc. Chem. Soc.: Lond.* **1962**, 386-387.
- (3) Negoro, M.; Kagawa, A.; Tateishi, K.; Tanaka, Y.; Yuasa, T.; Takahashi, K.; Kitagawa, M. Dissolution Dynamic Nuclear Polarization at Room Temperature Using Photoexcited Triplet Electrons. *J. Phys. Chem. A* **2018**, 122, 4294-4297.
- (4) Chiarelli, R.; Novak, M. A.; Rassat, A.; Tholence, J. L. A ferromagnetic transition at 1.48 K in an organic nitroxide. *Nature* **1993**, 363, 147-149.
- (5) Uchida, Y.; Ikuma, N.; Tamura, R.; Shimono, S.; Noda, Y.; Yamauchi, J.; Aoki, Y.; Nohira, H. Unusual intermolecular magnetic interaction observed in an all-organic radical liquid crystal. *J. Mater. Chem.* **2008**, 18, 2950-2952.
- (6) Uchida, Y.; Suzuki, K.; Tamura, R.; Ikuma, N.; Shimono, S.; Noda, Y.; Yamauchi, J. Anisotropic and Inhomogeneous Magnetic Interactions Observed in All-Organic Nitroxide Radical Liquid Crystals. *J. Am. Chem. Soc.* **2010**, 132, 9746-9752.
- (7) Nakagami, S.; Akita, T.; Kiyohara, D.; Uchida, Y.; Tamura, R.; Nishiyama, N. Molecular Mobility Effect on Magnetic Interactions in All-Organic Paramagnetic Liquid Crystal

with Nitroxide Radical as a Hydrogen-Bonding Acceptor. *J. Phys. Chem. B* **2018**, *122*, 7409-7415.

- (8) Tamura, R.; Uchida, Y.; Suzuki, K. In *Handbook of Liquid Crystals, 2nd Edition*, Goodby, J. W.; Collings, P. J.; Kato, T.; Tschierske, C.; Gleeson, H.; Raynes, P.; Vill V., Ed.; Magnetic Properties of Organic Radical Liquid Crystals and Metallomesogens; John Wiley & Sons, New York, 2014; Vol. 8, Chapter 28, 1-28.
- (9) Percival, P. W.; Hyde, J. S. Saturation-recovery measurements of the spin-lattice relaxation times of some nitroxides in solution. *J. Magn. Reson.* **1976**, *23*, 249-257.
- (10) Bloembergen, N.; Morgan, L. O. Proton Relaxation Times in Paramagnetic Solutions. Effects of Electron Spin Relaxation. *J. Chem. Phys.* **1961**, *34*, 842-850.
- (11) Thouless, D. J.; Anderson, P. W.; Palmer, R. G. Solution of 'Solvable model of a spin glass'. *Philos. Mag.* **1977**, *35*, 593-601.
- (12) Palmer, R. G.; Pond, C. M. Internal field distributions in model spin glasses. *J. Phys. F: Metal Phys.* **1979**, *9*, 1451-1459.
- (13) Edwards, S. F.; Anderson, P. W. Theory of spin glasses. *J. Phys. F: Metal Phys.* **1975**, *5*, 965-974.
- (14) Bayly, C. I.; Cieplak, P.; Cornell, W. D.; Kollman, P. A. A well-behaved electrostatic potential based method using charge restraints for deriving atomic charges: The RESP method. *J. Phys. Chem.* **1993**, *97*, 10269-10280.
- (15) Frisch, M. J.; Trucks, G. W.; Schlegel, H. B.; Scuseria, G. E.; Robb, M. A.; Cheeseman, J. R.; Scalmani, G.; Barone, V.; Mennucci, B.; Petersson, G. A.; Nakatsuji, H.; Caricato, M.; Li, X.; Hratchian, H. P.; Izmaylov, A. F.; Bloino, J.; Zheng, G.; Sonnenberg, J. L.; Hada, M.; Ehara, M.; Toyota, K.; Fukuda, R.; Hasegawa, J.; Ishida, M.; Nakajima, T.; Honda, Y.; Kitao, O.; Nakai, H.; Vreven, T.; Montgomery, J. A. Jr.; Peralta, J. E.; Ogliaro, F.; Bearpark, M.; Heyd, J. J.; Brothers, E.; Kudin, K. N.; Staroverov, V. N.; Kobayashi, R.; Normand, J.; Raghavachari, K.; Rendell, A.; Burant, J. C.; Iyengar, S. S.; Tomasi, J.; Cossi, M.; Rega, N.; Millam, J. M.; Klene, M.; Knox, J. E.; Cross, J. B.;

- Bakken, V.; Adamo, C.; Jaramillo, J.; Gomperts, R.; Stratmann, R. E.; Yazyev, O.; Austin, A. J.; Cammi, R.; Pomelli, C.; Ochterski, J. W.; Martin, R. L.; Morokuma, K.; Zakrzewski, V. G.; Voth, G. A.; Salvador, P.; Dannenberg, J. J.; Dapprich, S.; Daniels, A. D.; Farkas, Ö.; Foresman, J. B.; Ortiz, J. V.; Cioslowski, J.; Fox, D. J. Gaussian 09, Revision D.01, Gaussian, Inc., Wallingford CT, (2009).
- (16) Wang, J.; Wolf, R. M.; Caldwell, J. W.; Kollman, P. A.; Case, D. A. Development and testing of a general amber force field. *J. Comput. Chem.* **2004**, *25*, 1157-1174.
- (17) Ikuma, N.; Tamura, R.; Shimono, S.; Kawame, N.; Tamada, O.; Sakai, N.; Yamauchi, J.; Yamamoto, Y. Magnetic properties of all-organic liquid crystals containing a chiral five-membered cyclic nitroxide unit within the rigid core. *Angew. Chem. Int. Ed.* **2004**, *43*, 3677-3682.
- (18) Berendsen, H. J.; Postma, J. V.; van Gunsteren, W. F.; DiNola, A. R. H. J.; Haak, J. R. Molecular dynamics with coupling to an external bath. *J. Chem. Phys.* **1984**, *81*, 3684-3690.
- (19) Hoover, W. G. Canonical dynamics: Equilibrium phase-space distributions. *Phys. Rev. A* **1985**, *31*, 1695-1697.
- (20) Parrinello, M.; Rahman, A. Polymorphic transitions in single crystals: A new molecular dynamics method. *J. Appl. Phys.* **1981**, *52*, 7182-7190.
- (21) Hess, B.; Bekker, H.; Berendsen, H. J.; Fraaije, J. G. A linear constraint solver for molecular simulations. *J. Comput. Chem.* **1997**, *18*, 1463-1472.
- (22) Dvinskikh, S. V.; Furó, I.; Zimmermann, H.; Maliniak, A. Anisotropic Self-Diffusion in Thermotropic Liquid Crystals Studied by 1H and 2H Pulse-Field-Gradient Spin-Echo NMR. *Phys. Rev. E* **2002**, *65*, 061701.
- (23) Cho, D.; Ko, K. C.; Lee, J. Y. Quantum chemical approaches for controlling and evaluating intramolecular magnetic interactions in organic diradicals. *Int. J. Quantum Chem.* **2016**, *116*, 578-597.

- (24) Khafizov, N. R.; Madzhidov, T. I.; Kadkin, O. N.; Tamura, R.; Antipin, I. S. Quantum chemical calculation of exchange interactions in supramolecularly arranged N, N'-dioxy-2,6-diazaadamantane organic biradical. *Int. J. Quantum Chem.* **2016**, *116*, 1064-1070.
- (25) Ravat, P.; Baumgarten, M. Positional Isomers of Tetramethoxypyrene-based Mono-and Biradicals. *J. Phys. Chem. B* **2015**, *119*, 13649-13655.
- (26) Yamanaka, S.; Kawakami, T.; Nagao, H.; Yamaguchi, K. Effective exchange integrals for open-shell species by density functional methods. *Chem. Phys. Lett.* **1994**, *231*, 25-33.
- (27) Luyten, P. R.; Bulthuis, J.; Bove, W. M. M. J.; Plomp, L. The dynamical behavior of a small probe molecule dissolved in a nematic liquid crystal studied by NMR. *J. Chem. Phys.* **1983**, *78*, 1712-1721.
- (28) Nayeem, A.; Freed, J. H. ESR study of the dynamic molecular structure of a reentrant nematic liquid crystal. *J. Phys. Chem.* **1989**, *93*, 6539-6550.
- (29) Kawai, A.; Obi, K. First observation of a radical-triplet pair mechanism (RTPM) with doublet precursor. *J. Phys. Chem.* **1992**, *96*, 52-56.
- (30) Hertz, J.; Krogh, A.; Palmer, R. G. *Introduction to the Theory of Neural Computation*, Addison-Wesley Longman Publishing Co., Inc., Boston, 1991.